



Received: 15/12/2022
Accepted: 22/12/2022

Anales de Edificación
Vol. 8, Nº3, 47-53 (2022)
ISSN: 2444-1309
Doi: 10.20868/ade.2022.5098

Modelo CFD con validación de campo para el estudio de los alcances de efectividad de técnicas de mitigación de radón por despresurización. CFD model with field validation for the study of the effectiveness of radon mitigation techniques by depressurisation.

Isabel Sicilia^{a,b}; Borja Frutos^a; Carmen Alonso^a; Fernando Martín-Consuegra^a; Fernando de Frutos^a; Ignacio Oteiza^a; Carlos Sainz^b; Luis S. Quindós^b

^a Instituto de Ciencias de la Construcción Eduardo Torroja. Consejo Superior de Investigaciones científicas. (IETcc-CSIC). Madrid, España. (i.sicilia@ietcc.csic.es; borjafv@ietcc.csic.es; c.alonso@ietcc.csic.es; martin-consuegra@ietcc.csic.es; fernando.defrutos@ietcc.csic.es; ioteiza@ietcc.csic.es)

^b Universidad de Cantabria. España. (carlos.sainz@unican.es; luis.quindos@unican.es)

Resumen— La reducción de niveles de gas radón en el interior de edificios supone un desafío debido a las diferentes características de terrenos y sistemas constructivos, especialmente en edificios ya construidos. El artículo presenta los avances en el desarrollo de un modelo de simulación en COMSOL Multiphysics para el estudio de movimientos de gas radón bajo solera. En primer lugar, se estudian los parámetros que afectan a los movimientos del gas, como las características de materiales, terreno, sistemas constructivos y potencia de extracción. Posteriormente, partiendo de una base experimental previa, se calibra un modelo simplificado de forma que se puedan aproximar los resultados del modelo de simulación a los recabados en el modelo real. El presente trabajo se enmarca en el proyecto Radon_Flow (PID2019-109898RB-I00) desarrollado en el Instituto Eduardo Torroja, perteneciente al Consejo Superior de Investigaciones Científicas de España.

Palabras clave— Radón; Mitigación; Modelo CFD; Eficacia; Despresurización.

Abstract— Reducing radon gas levels inside buildings is a challenge due to the different characteristics of soils and construction systems, especially in existing buildings. The paper presents the progress in the development of a simulation model in COMSOL Multiphysics for the study of radon gas movements under screed. Firstly, the parameters that affect gas movements, such as the characteristics of materials, soil, construction systems and extraction power, are studied. Subsequently, starting from a previous experimental basis, a simplified model is calibrated so that the results of the simulation model can be approximated to those obtained in the real model. This work is part of the Radon_Flow project (PID2019-109898RB-I00) developed at the Eduardo Torroja Institute, belonging to the Spanish National Research Council (CSIC).

Index Terms— Radon; Mitigation; CFD model; Effectiveness; Depressurisation.

I. INTRODUCTION

RADON gas is a naturally occurring radioactive gas resulting from the decay of radium and uranium present in the ground. Weighing more than air and with a half-life of 3.8

days, radon penetrates buildings and tends to accumulate on the lower floors (Cinelli et al., 2019; Quindós Poncela, 1995). As it disintegrates, it generates alpha particles, which enter the human respiratory tract, and is considered by the World Health Organisation to be one of the main causes of lung cancer

(WHO, 2009). It is currently considered necessary to establish mitigation measures so that the concentration does not exceed 300 Bq/m³ in living spaces (EURATOM, 2013; CTE, 2019).

The removal of radon gas from buildings is a global problem. In recent years, the need for its control has been incorporated into the building regulations of different European countries, such as the Spanish Technical Building Code (CTE, 2019). Among the most effective solutions for reducing high radon levels are under-slab depressurisation techniques (Frutos, 2011; Pacheco-Torgal, 2012). These techniques consist of maintaining a lower pressure than that existing inside the building in those surfaces located under the floor slab of basements and floors in contact with the ground. In this way, the air tends to move down the pressure gradient towards the space where the pressure is lower, thereby reducing the ingress of contaminated air into the building. Depressurisation is usually created by the incorporation of mechanical extraction systems, which take the air from the ground and expel it to the outside, where the radon concentration is diluted.

For the under-slab depressurisation system to be effective, the negative pressure field should ideally cover the entire area under the building. In new buildings it is possible to provide for the formation of a more permeable space underneath (e.g., a gravel bed) in the design, which allows for a greater extension of the negative pressure field with respect to the interior. However, in existing buildings, radon gas removal is more complicated and the choice of suction points, extraction systems and extraction power must be made according to the composition and permeability of the space under the slab. The problem is aggravated by the presence of poorly permeable materials and structural foundations, which impede the continuity of air flows.

This work is part of the Radon_Flow project "Porous aggregates and screeds for protection against radon gas", developed at the Eduardo Torroja Institute. Based on the pressure data collected in experiments on a full-scale slab model, progress is being made in defining the necessary parameters for the creation of a simulation model with the COMSOL Multiphysics software. This model will allow the study of different materials and procedures for radon gas removal. The empirically collected data were presented in October 2021 at the International Conference Construction, Energy, Environment and Sustainability CEES 2021 in Coimbra (Portugal) (Sicilia et al., 2021). Based on these data, a COMSOL slab model is validated, using as a control element the differential pressures measured at different points of the experimental slab, with different extraction systems.

II. THEORETICAL FRAME

Radon gas atoms are generated both within soil grains and in building materials containing radium and/or uranium. Once generated, they move to the surface by three processes: emanation, transport, and exhalation (Cinelli et al., 2019). During emanation, radon generated inside the grain moves into the air in the surrounding pores of the soil. Once there, transport takes place by diffusion and advection processes, which move

the radon atoms to the surface. Finally, the radon gas is exhaled into the free air of the atmosphere. Transport by diffusion and advection occurs both in the natural ground and through the building materials in contact with it. Radon enters the interior through surfaces in contact with the ground, as well as through existing cracks and some elements of the sewage system.

The concentration variation over time is represented by the following equation (Clements, 1974):

$$\frac{\partial \varepsilon C}{\partial t} = D \nabla^2 C + \frac{k}{\mu} C \nabla P - \lambda \varepsilon C + \varepsilon G \quad (1)$$

The first term describes the diffusion process, with C being the radon concentration in the medium [Bq/m³], D the diffusion coefficient in the soil [m²/s], and ε the porosity of the medium, with a range between 0 and 1. The second term represents the advection process, with k being the intrinsic permeability of the porous medium, μ the dynamic viscosity of the gas in the soil [Pa s], and ∇P the pressure difference between the porous medium and the outside [Pa]. The last two terms correspond to the radioactive decay, where λ is the decay constant of 222Rn [s⁻¹], and G is the radon generation in the soil pores [Bq m⁻³·s⁻¹].

The first part of the modelling, developed in the present work, is focused on the advection processes, described by Darcy's Law (Jiranek et al., 2007) (second term of equation 1). The approximation to the operation of the real system is carried out considering that radon ingress into a dwelling is reduced if the pressures under the slab are lower than those in the space above (HC, 2010). The study includes the analysis of different parameters that may affect the transmission of pressures: average extraction velocity, permeability and porosity of the soil, the existence of cracks in the slab and their definition characteristics, the existence of intermediate foundations that may interrupt the flow, and the existence or not of a gravel layer under the slab.

To be able to compare results, several control points are established in the simulation model, coinciding with the measurement points established in the slab of the experimental model. On the other hand, in the experimental prototype, the extraction speed and flow rate control has been previously carried out to establish the different working frames (sets).

The software used, COMSOL Multiphysics, develops the advection transport equation in two parts (COMSOL, 2020): a velocity calculation as a function of porosity, permeability, dynamic viscosity, and pressure gradient (equation 2), and a flow calculation from the density applied to the flow represented by the velocity (equation 3).

$$\vec{u} = \frac{k}{\mu} \nabla P \quad (2)$$

$$\nabla \cdot (\rho \vec{u}) = Q_m \quad (3)$$

The calculations are carried out in stationary mode, considering that once the extraction system is started up, pressures tend to stabilise.

III. MATERIALS AND METHODS

The experiments are carried out on a concrete slab located within the facilities of the Eduardo Torroja Institute in Arganda del Rey. With a surface area of 64 m², the slab is divided into 4 quadrants, perimeter kerbs and an intermediate spacing simulating an internal foundation. Several tests are carried out to see the influence of the size of the surrounding soil on the results of the model. The aim is to use the minimum possible terrain volume to reduce computational times, but without losing accuracy in the calculation. The results determine a minimum ground surface bounded by an area of 5 metres with respect to the slab edges and a depth of 10 metres.

The starting condition is a pressure of 0 Pa both at the surface and in the volume of the soil. Table 1 shows the default properties assigned to each of the materials. For the simulations with cracks, the existence of a concrete shrinkage fracture is considered, which would take place perimetrically at all joints of the quadrants with the foundation kerbs.

The slab is equipped with a system of tubes that allows the placement of a differential pressure measurement sensor system developed by the Torres Quevedo Institute of Physical Technologies (Sicilia et al., 2019). To carry out the depressurisation experiments, the slab (Fig. 1) is equipped with an extraction system by means of two independently operating sumps (marked in Fig. 1 as External and Internal sump), and central points for the arrangement of an autonomous extraction system (in Fig. 1, Cylindrical collectors). In the analysis of the present work, only the extraction from the central points will be considered.

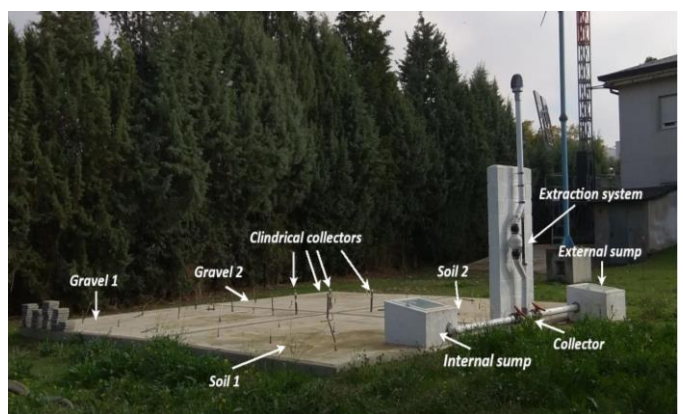


Fig. 1. Experimental device. Full-scale slab in Arganda del Rey. Source: Sicilia et al., 2021.

Fig. 3 shows the geometry of the model used, which represents the experimental slab. It has four quadrants, perimeter kerbs and an intermediate spacing simulating an internal foundation. Several tests are carried out to see the influence of the size of the surrounding soil on the results of the model. The aim is to use the minimum possible terrain volume to reduce computational times, but without losing accuracy in the calculation. The results determine a minimum ground surface bounded by an area of 5 metres with respect to the slab edges and a depth of 10 metres.

The starting condition is a pressure of 0 Pa both at the surface and in the volume of the soil. Table 1 shows the default properties assigned to each of the materials. For the simulations with cracks, the existence of a concrete shrinkage fracture is considered, which would take place perimetrically at all joints of the quadrants with the foundation kerbs.

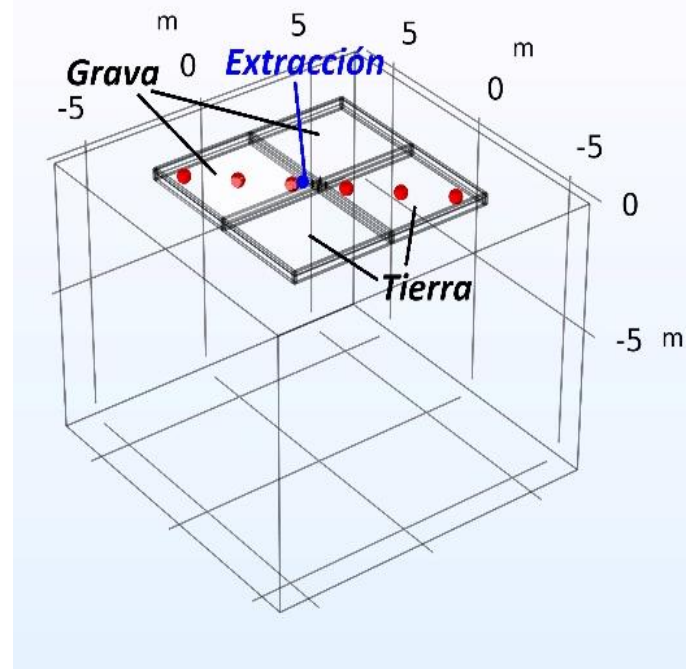


Fig. 3. Simulation model. In red, the measurement points whose data will be used for the elaboration of the graphs. In blue, extraction point.



a)



b)

Fig. 2. (a) Air extraction process for depressurisation. Polystyrene enclosures contain the differential pressure sensors. b) Differential pressure sensor module.

TABLE I
DEFAULT VALUES OF MATERIALS USED FOR SIMULATION STUDIES

	Porous matrix		Fluid	
	Permeability	Porosity	Dynamic viscosity	Density
	[m ²]		Kg/(m·s)	Kg/m ³
Air	7.5 E-7	1	1.74 E-6	1.293
Ground	1 E-11	0.25	1.74 E-6	1.293
Concrete	1 E-15	0.2	1.74 E-6	1.293
Gravel	5 E-8	0.4	1.74 E-6	1.293
Crack	1 E-8	1	1.74 E-6	1.293

The simulations are carried out in two phases. In the first phase, the basic parameters for the operation of the model are defined, varying the dimensions of the terrain, the definition of its walls, or the inclusion of gravity effects. In the second phase, parametric sweeps are performed to analyse the influence of each of the parameters that can be found in real buildings: permeability of the terrain, presence of fractures, different points and flow velocities/extraction flows, etc.

Finally, the data are compared with the data collected on the slab in order to perform a calibration of the model.

IV. RESULTS AND DISCUSSION

This article presents the results of the simulation of the generation of a pressure field by the extraction of air from one of the quadrants of the slab built on gravel (Gravel 1 quadrant). The points on a cut-offline between the outer corner of the extraction quadrant, Gravel 1, and the outer corner of the diagonally symmetric quadrant, Earth 2 (Fig. 3) will be used as a reference for the graphs.

A. Initial values of actual experimentation

For the analysis of the behaviour of the slab, the values measured on the actual slab will be taken. The extraction is performed at the maximum flow velocity measured in the quadrant (Gravel 1, V4), with a value of 3.97 m/s (table 2). A more complete analysis of the field data can be found in the article (Sicilia et al., 2021).

B. Variation of extraction speed.

A study is carried out on the model by varying the extraction velocities with suction in the Gravel 1 quadrant.

TABLE III
AVERAGE VELOCITY AND FLOW RATE PARAMETERS OBTAINED IN THE EXPERIMENTS ON THE REAL SLAB

Type of surface under quadrant		V4	Q4	V3	Q3	V2	Q2	V1	Q1
		[m/s]	[m ³ /h]						
SETUP 1	Floor 1	2.21	62.49	1.82	51.46	1.38	39.02	1.01	28.56
SETUP 2	Soil 2	2.16	61.07	1.04	29.41	1.42	40.15	1.80	50.89
SETUP 3	Gravel 1	3.97	112.25	3.35	94.72	2.96	83.69	2.30	65.03
SETUP 4	Gravel 2	3.80	107.44	3.28	92.74	2.66	75.21	2.20	62.20

TABLE II
PRESSURE DISTRIBUTION IN THE EXPERIMENTAL SLAB. EXTRACTION IN GRAVEL QUADRANT 1, AT MAXIMUM VELOCITY AND FLOW RATE.

SETUP 3 - V4					
-82.0	-89.7	-90.4	-25.3	-26.1	-7.2
-87.3	-92.1	-91.6	-25.9	-25.6	-26.6
-90.0	-91.9	-96.4	-25.6	-26.6	-26.9
-16.6	-29.2	-30.2	-16.2	-12.3	-10.9
-6.7	-16.6	-17.2	-11.5	-9.3	-7.7
-6.5	-7.3	-7.8	-9.4	-7.3	-4.6

The structure is dimensioned for a dead load of 5.95 kN/m² and a live load of 1.5 kN/m². A frame is chosen from this construction in order to perform its structural analysis under the post-earthquake fire action using the ISO 834 standard fire (1999) for 4 hours. Fig. 8 illustrates the geometry of the frame as well as the fire scenario. Only three sides of the structural elements were exposed to fire.

Fig. 4 shows how, thanks to the gravel layer, the pressure field expands rapidly to all points in that quadrant, with very little pressure loss along the entire diagonal. The pressure generated can penetrate the central foundation in the ground but is rapidly lost as it moves away from the point of extraction to the point of having values close to 0 at a distance of 6 metres. It can also be observed that the pressure is lost very quickly as it crosses the foundation lines, both the inner and the outer ones.

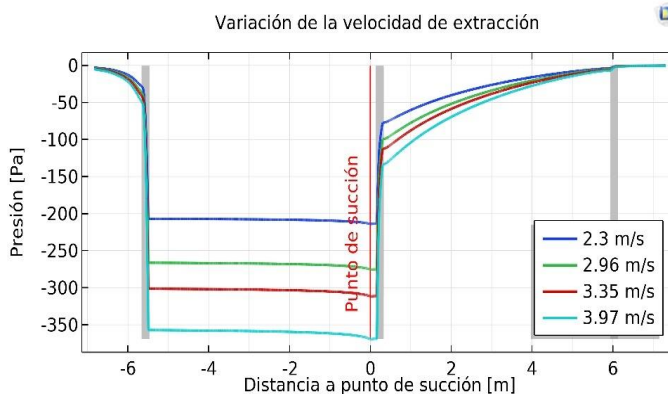


Fig. 4. Variation of the extraction speed and pressure measurement on the G1-T2 diagonal.

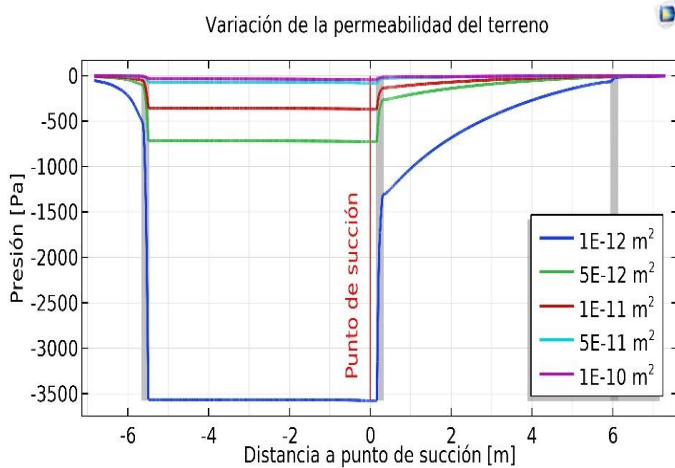


Fig. 5. Permeability variation and pressure measurement on the G1-T2 diagonal.

C. Variation of soil permeability

Typical values for a soil in its natural state range from 4. 10-11 m² for sandy soils to 10-14 m² for clay soils (Nazaroff et al., 1988). We limit the permeability analysis to 10-12, corresponding to a loamy soil. Very poorly permeable soils confine the gravel layer, increasing the pressure in the gravel layer to extremely high values. Reducing the permeability of the soil from 10-11 to 10-12 generates a 10 times higher pressure field in the gravel layer.

D. Crack width variation

Cracks usually occur in the joints of building elements. As they have a very high permeability, much higher than that of the building elements, they are a source of radon ingress into the interiors. Fig. 6 shows how the pressure field distribution is affected by the presence of a perimeter crack inside the slab quadrants. The default permeability of the crack is estimated at 10-8 m², assuming a crack with discontinuity and the presence of dust and filler materials in some of its sections.

If we compare the pressure values of the minimum crack with those obtained in the slab without cracks (Fig. 4, maximum velocity), we see that a small crack of one hundredth of a millimetre can reduce the pressure field in the gravel layer by about 5%. As the size of the crack increases, the system becomes less and less effective and the pressure range is drastically reduced.

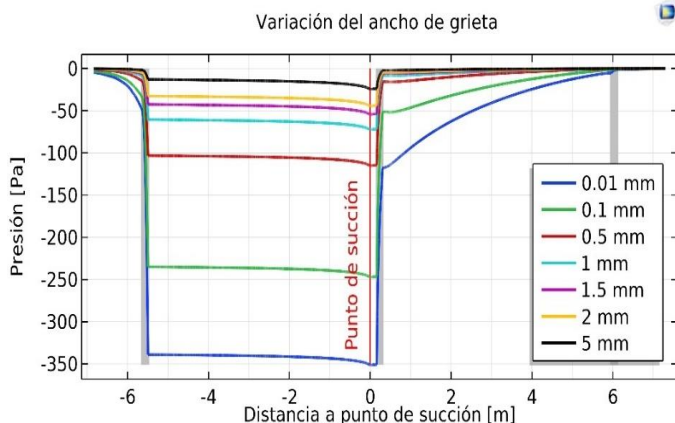


Fig. 6. Variation of the width of a perimeter fracture at quadrant edges and pressure measurement on the G1-T2 diagonal.

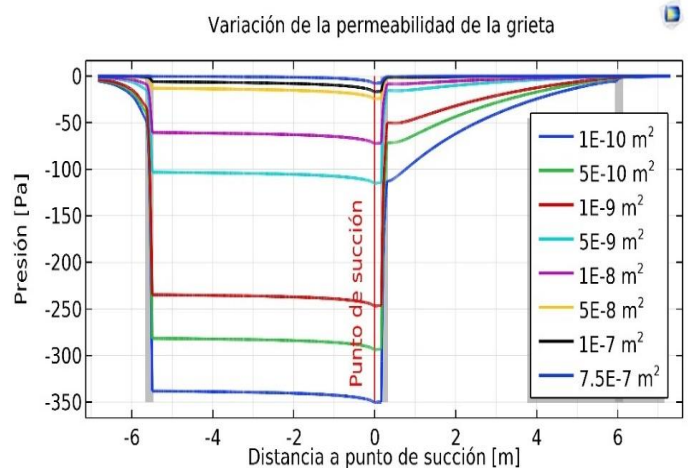


Fig. 7. Variación de la permeabilidad de una fractura perimetral en los bordes de los cuadrantes y medición de presión en la diagonal G1-T2.

E. Variation of crack permeability

Crack permeability represents the continuity of cracks along the entire fracture. In the case of a clean, open crack, it would have the same permeability as the air of which it is composed. A dirty crack, with filler materials or discontinuities, would have a lower permeability. The analysis is carried out with a crack width of 1 mm. As can be seen in Fig. 7, the permeability of the crack is decisive in establishing its influence on the pressure system.

F. Model calibration

Based on the above parameters, a first calibration of the model is carried out. In the visual examination, small cracks are visible on the surface, although they are not distributed around the perimeter, and their continuity in depth is unknown. We adjust the model with a crack of 0.1 mm and permeability 10-8 m², as well as a ground permeability of 3.5. 10-11 m². We extract data from all quadrants for comparison with the empirical data (table 4).

As can be seen by comparing table 2 and table 4, the values in both gravel and earth quadrants are quite similar. Through simulation we can understand in more detail how the pressure transmission process takes place (Fig. 8).

TABLE IV
 PRESSURE DISTRIBUTION IN THE SLAB MODEL. EXTRACTION IN GRAVEL QUADRANT 1, AT MAXIMUM VELOCITY AND FLOW RATE.

-87.4	-87.8	-88.0	-23.6	-23.4	-23.2
-87.9	-88.6	-89.3	-23.7	-23.4	-23.2
-88.2	-89.4	-92.1	-23.7	-23.4	-23.2
-31.3	-38.92	-34.9	-20.1	-14.7	-10.2
-13.1	-17.86	-16.6	-12.2	-9.2	-5.6
-5.7	-7.88	-7.6	-6.9	-4.8	-2.9

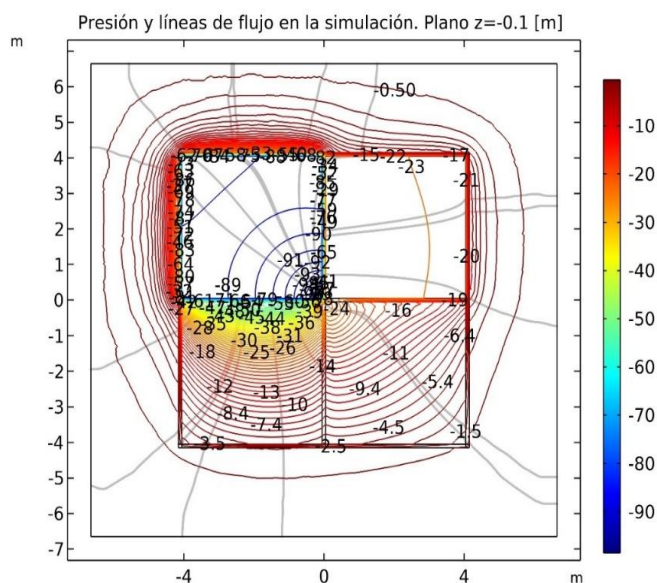


Fig. 8. Distribution of pressures and flows in the plane below the slab surface ($z=-0.1$ m). The two upper quadrants correspond to the quadrants built on gravel, and the two lower quadrants to those directly supported on the ground.

V. CONCLUSIONS

As can be seen from the results, a fundamental factor when designing a depressurisation system is the permeability of the space under the slab. Fig. 5 shows how a low permeable material would help to increase pressure transmission if there is a permeable layer (gravel) under the slab but would be very ineffective in spaces where there is no permeable surface.

The presence of foundations means that the flow must pass through or around a very low permeable material, such as concrete, having a similar effect to that of the ground, with a large pressure drop. In the prototype, the foundation has been designed as a continuous element, but the development of simulation models would make it easier to analyse the effect of discontinuous elements or those containing a space of greater permeability that allows the flow to pass through.

On the other hand, we found that the condition of the slab, especially with regard to the joints between construction elements, plays a decisive role in the proper functioning of the depressurisation systems. In the simulation of the slab, we observed that with clean cracks larger than 1 mm, it is not possible to guarantee depressurisation at all points of the slab. The influence would be reduced in the case of dirty or poorly permeable cracks. However, the difficulty of locating and determining the characteristics of all cracks makes it advisable to establish efficient sealing systems by default.

By simulating the flows and pressures, we can determine the pressure plane generated under the building (Fig. 8), and we can detect possible points where the appropriate pressure is not reached. Similarly, the analysis of the simulation allows us to check the influence of the characteristics of the building form, such as the presence of gravel or cavities under the slab and the barriers formed by the foundations (Fig. 9). The design of the suction system must be such that it allows the best distribution of pressures.

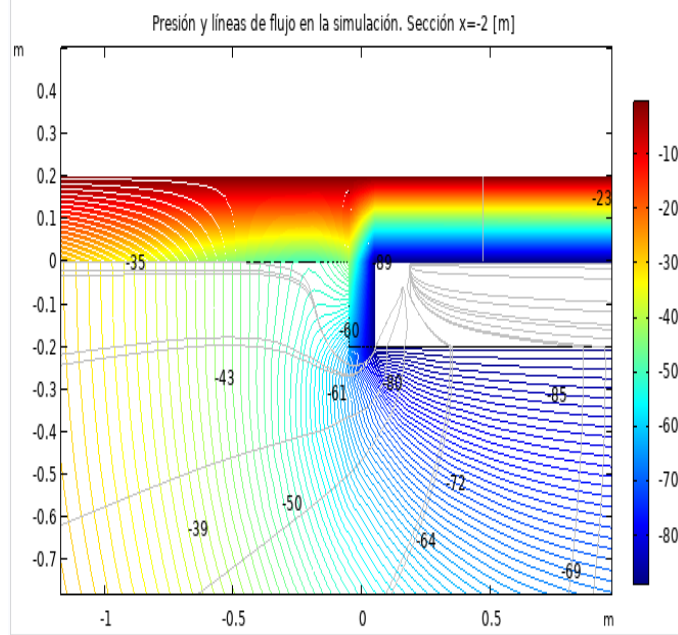


Fig. 9. Distribution of pressures in the inner foundation passage.

The study presented in this article represents a first approximation to the analysis of radon gas movements under the sill, being in many cases sufficient the establishment of a depressurisation layer. However, further development of the transport model is needed to include radon diffusion, radon generation and radon decay terms. For some sites and buildings these terms are critical in the design of a mitigation system and are essential for estimating the effective reduction of indoor radon concentrations.

ACKNOWLEDGEMENTS

This research is funded by the Spanish National Research Council (CSIC), within the RADON_FLOW project (PID2019-109898RB-I00). The study has been carried out at the Instituto de Ciencias de la Construcción Eduardo Torroja (IETcc), in Madrid, Spain.

REFERENCES

- G. Cinelli, M. De Cort, T. Tollefsen, M. Achatz, J. Ajtić, C. Ballabio, I. Barnett, F. Bochicchio, P. Borelli, P. Bossew, R. Braga, E. Brattich, A. Briganti, C. Carpentieri, C. Castellani, M. Castelluccio, E. Chiaberto, G. Ciotoli, C. Coletti, A. Cucchi, Z. Daraktchieva, C. Di Carlo, J. De France, B. Dehandschutter, F. Domingos, T. Dudar, J. Elio, P. Falletti, A. Ferreira, I.E. Finne, C. Fontana, I. Fuente Merino, G. Galli, M. Garcia-Talavera, O. German, C. Grossi, V. Gruber, J. Gutierrez-Villanueva, M. Hansen, M.A. Hernandez Ceballos, M. Hoffmann, S. Hurst, G. Iurlaro, K. Ivanova, V. Jobbagy, A. Jones, G. Kovalenko, K. Kozak, R. Lawley, R. Lehné, B. Lister, S. Long, C. Lucchetti, M. Magnoni, M. Matolin, J. Mazur, C. Mazzoli, J. McLaughlin, M. Mollo, D. Mostacci, S. Mundigl, D. Nesbor, L. Neves, M. Neznal, J. Nikolov, P. Nilsson, A. Nogarotto, A. Onischenko, A. Orgiazzi, P. Pacherová, P.

- Panagos, A. Pereira, M.D.R. Perez, V. Pokalyuk, D. Pressyanov, L.S. Quindós Poncela, W. Ringer, F. Rossi, M. Sangiorgi, R. Sassi, Z. Simic, P. Smedley, S. Socciarelli, M. Soligo, S. Stoulos, K. Szabo, K. Täht-Kok, N. Todorović, R. Tolton, P. Tuccimei, T. Turtiainen, A. Tye, V. Udovicic, A. Vasilyev, G. Venoso, S. Verdelocco, V. Verkhovtsev, M. Voltaggio, O. Zhukova, M. Zhukovsky, European atlas of Natural radiation, 2019. <https://doi.org/10.2760/46388>.
- W.E. Clements, M.H. Wilkening, Atmospheric pressure effects on 222Rn transport across the Earthair interface, 1974. <https://doi.org/10.1029/JC079i033p05025>.
- R. Manual, COMSOL Multiphysics® v. 5.5 Reference Manual, (2018) 1742.
- EURATOM, Unión Europea, DIRECTIVA 2013/59/EURATOM del Consejo de 5 de diciembre de 2013, por la que se establecen normas de seguridad básicas para la protección contra los peligros derivados de la exposición a radiaciones ionizantes., D. Of. La Unión Eur. (2014) W.W. Nazaroff, B.A. Moed, R.G. Sextro, Soil as a Source of Indoor Radon, Generation, Migration, and Entry, Radon Its Decay Prod. Indoor W.W. Nazaroff, A.V. Nero Jr. (1988) 57–112.
- M. de Fomento, CTE. Sección DB HS-6. Protección frente a la exposición al radón, in: Código Técnico La Edif., España, 2019: pp. 1–49.
- B. Frutos, M. Olaya, J.L. Esteban, Sistemas de extracción como técnicas constructivas para evitar la entrada de gas radón en las viviendas, Inf. La Construcción. 63 (2011) 23–36.
- B. Frutos, I. Sicilia, O. Campo, S. Aparicio, M. Gonz, R. Daniel, M. González, J.J. Anaya, D. Rábago, C. Sainz, A full-scale experimental study of sub-slab pressure fields induced by underground perforated pipes as a soil depressurisation technique in radon mitigation, J. Environ. Radioact. 225 (2020) 106420. <https://doi.org/10.1016/j.jenvrad.2020.106420>.
- M. Fuente, E. Muñoz, I. Sicilia, J. Goggins, L.C. Hung, B. Frutos, M. Foley, Investigation of gas flow through soils and granular fill materials for the optimisation of radon soil depressurisation systems, J. Environ. Radioact. 198 (2019) 200–209. <https://doi.org/10.1016/j.jenvrad.2018.12.024>.
- M. Jiranek, Z. Svoboda, Numerical modelling as a tool for optimisation of sub-slab depressurisation systems design, Build. Environ. 42 (2007) 1994–2003. <https://doi.org/10.1016/j.buildenv.2006.04.002>.
- Health Canada, Reducing Radon Levels in Existing Homes. A Canadian Guide for Professional Contractors, (2010) 70.
- F. Pacheco-Torgal, Indoor radon: An overview on a perennial problem, Build. Environ. 58 (2012) 270–277. <https://doi.org/10.1016/j.buildenv.2012.08.004>.
- L. Quindós-Poncela, Radon: Un gas radioactivo de Origen Natural en su Casa, Universida, Santander, 1995.
- I. Sicilia, Isabel; Frutos, Borja; Sáinz, Carlos; Quindós, Luis, Alonso, Carmen; Martín-Consuegra, Fernando; de Frutos, Fernando; Pérez, Gloria; Oteiza, Study of porous layers for the establishment of design parameters applied to depressurization techniques for radon mitigation, CEES 2021- Int. Conf. Constr. Energy, Environ. Sustain. (2021) 31. https://epic.awi.de/32157/2/Book_of_Abstracts_ART_AP_ECS.pdf.
- I. Sicilia, S. Aparicio, B. Frutos, E. Muñoz, M. González, J.J. Anaya, A Multisensor System for the Characterization of the Field Pressure in Terrain. Accuracy, Response, and Adjustments, Sensors. 19 (2019) 3942. <https://doi.org/10.3390/s19183942>.
- WHO, Who Handbook on Indoor Radon - A Public Health Perspective, World Heal. Organ. (2009) 110 p. <https://doi.org/10.1080/00207230903556771>.
- L13/1-73. <http://www.boe.es/doue/2014/013/L00001-00073.pdf>.



Reconocimiento – NoComercial (by-nc): Se permite la generación de obras derivadas siempre que no se haga un uso comercial. Tampoco se puede utilizar la obra original con finalidades comerciales.